SF2A 2024
M. Béthermin, K. Baillié, N. Lagarde, J. Malzac, R.-M. Ouazzani, J. Richard, O. Venot, A. Siebert (eds)

MAGNETO-ROTATIONAL SUPERNOVA EXPLOSIONS: A COMPARISON BETWEEN STATE-OF-THE-ART NUMERICAL MODELS

M. Bugli[1,2,3], J. Guilet[2], K. Kotake[4], L. Kovalenko[5], B. Müller[6], M. Obergaulinger[7], E. O'Connor[5], T. Takiwaki[8] and V. Varma[9]

Abstract. We present results from a code-comparison project which considers, for the first time, the modeling of a prototypical 3D magneto-rotational explosion realized with state-of-the-art CCSN numerical codes that use different grid geometries, gravity treatment, and neutrino-matter interactions. We show the impact that specific modeling choices have on the explosion dynamics, the shock propagation, the formation of the central compact object, the stability of the polar outflow, and the multi-messenger emission (neutrinos and gravitational waves) associated to a long GRB progenitor. The overall good agreement between completely independent codes showcases the maturity of the CCSN modeling community and the potential for more quantitative predictions related to outstanding stellar explosion models.

Keywords: core-collapse supernovae, magnetic fields, MHD, numerical simulations, multi-messenger astronomy

1 Introduction

The gravitational collapse of a massive star with a fast-rotating core sets the stage for the onset of magneto-rotational core-collapse supernovae (CCSN). The accreting central compact object is believed to be the central engine that can power up outstanding stellar explosions such as hypernovae and long gamma-ray bursts (GRB). Over the last decades magnetohydrodynamic numerical models of magnetized core-collapse have reached a high degree of complexity, as they include the effects of three-dimensional dynamics, nuclear equations of state, effects of general relativity, multi-dimensional neutrino transport schemes (Just et al. 2015; Müller & Janka 2015; Takiwaki et al. 2016; O'Connor & Couch 2018). This allows one in return to make quantitative predictions on the properties of the compact remnant(Kuroda & Umeda 2010; Obergaulinger & á. Aloy 2017; Bugli et al. 2020), the multi-messenger signatures of the explosion (Kuroda et al. 2020; Bugli et al. 2023; Powell et al. 2023; Shibagaki et al. 2024), the launching conditions of the relativistic jet (Takiwaki et al. 2009; Aloy & Obergaulinger 2021; Bugli et al. 2021), and the explosive nucleosynthesis of new heavy elements contributing to the chemical evolution of galaxies (Reichert et al. 2022, 2024; Zha et al. 2024). Such predictions depend crucially on the accuracy with which simulations can reproduce quantities such as the spin-down of the central proto-neutron star, the magnetic transport of angular momentum, the shock propagation through the stellar progenitor, and the neutron-richness of the ejecta. However, it remains still unclear to what extent the findings of numerical models of magneto-rotational explosions depend on the technical details of the specific tool used to produce them.

[1] Dipartimento di Fisica, Università di Torino, Torino, Italy
[2] Université Paris-Saclay, Université Paris Cité, CEA, CNRS, AIM, Gif-sur-Yvette, France
[3] INFN - Sezione di Torino, Torino, Italy
[4] Fukuoka University, Fukuoka, Japan
[5] The Oskar Klein Centre, Department of Astronomy, Stockholm University, Stockholm, Sweden
[6] Monash University, Clayton VIC, Australia
[7] Departament d'Astronomia i Astrofísica, Universitat de València, Burjassot (València), Spain
[8] National Astronomical Observatory of Japan, Mitaka, Japan
[9] Keele University, Staffordshire, United Kingdom

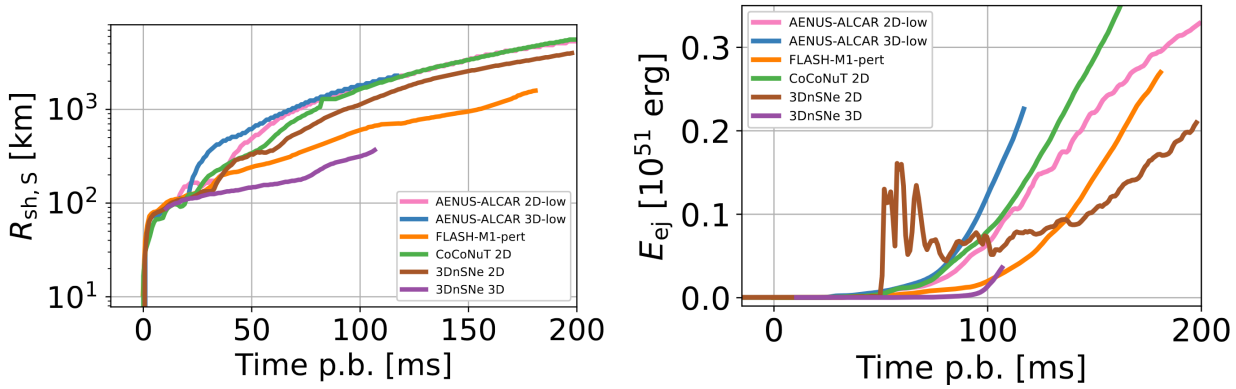

Fig. 1. Left: Shock radius expansion over time. **Right:** Evolution over time of the ejecta's energy.

In this work we present results from a comparative study involving 4 numerical codes (see Table 1) that aims at reproducing the explosion dynamics of a common magneto-rotational supernova progenitor and assessing the degree of consistency for results obtained with independently developed numerical tools. These codes are characterized by different choices for the grid structure (spherical, Cartesian), neutrino transport scheme (M1, IDSA, FMT), and gravity treatments.

2 Numerical setup

For our comparison we consider the widely used solar-metallicity stellar progenitor `s20` (Woosley & Heger 2007) with $M_{\rm ZAMS} = 20M_\odot$. The iron core has radius $R_{\rm Fe} = 1.7 \times 10^3$ km, mass $M_{\rm Fe} = 1.5M_\odot$ and central density $\rho_c = 5.8 \times 10^9$ g/cm^3. We assume a shellular initial rotation profile such as to have an inner region in solid-body rotation which then transitions to a constant specific angular momentum distribution. This is achieved by setting the angular velocity Ω to

$$\Omega(r) = \Omega_0 \frac{R_\Omega^2}{r^2 + R_\Omega^2}, \tag{2.1}$$

where r is the spherical radius, $\Omega_0 = 1$ rad/s is the central the angular velocity and $R_\Omega = 1000$ km is the size of the inner region. For the initial magnetic field we consider a modified aligned dipole, whose components can be expressed in terms of the azimuthal component of the vector potential (in Heaviside-Lorentz units)

$$A^\phi = \frac{B_0}{2} \frac{R_0^3}{R_0^3 + r^3} r \sin\theta, \tag{2.2}$$

which produces a field of constant magnitude B_0 for $r \ll R_0$ and a standard dipolar field decaying as $r \propto^{-2}$ for $r \gg R_0$. We set $B_0 = 5 \times 10^{11}$ (which corresponds to a maximum magnetic field of $\sim 1.77 \times 10^{12}$ G in the progenitor's core) and $R_0 = 1000$ km. We seed the same small density perturbation at core bounce (which we identify as the time when the maximum density in the simulation reaches a local maximum) $\delta\rho = \epsilon\rho_0 \sin(2\theta)\cos\phi$, where ρ_0 is the unperturbed density profile and $\epsilon = 10^{-2}$ is the amplitude of the perturbation. This choice allows us to favor the fast development of the kink instability, having azimuthal order $m = 1$ and introducing the perturbation off the equatorial plane ($l = 2$).

Table 1. List of numerical codes and their main features.

Code Name	Grid Geometry	Neutrino Transport	Gravity
3DnSNe-IDSA (Takiwaki et al. 2016)	(r, θ, ϕ)	IDSA	Marek et al. (2006)
AENUS-ALCAR Just et al. (2015)	(r, θ, ϕ)	M1	Marek et al. (2006)
CoCoNuT-FMT (Müller & Janka 2015)	(r, θ, ϕ)	FMT	Müller et al. (2008)
FLASH-M1 (O'Connor & Couch 2018)	(x, y, z)	M1	Marek et al. (2006)

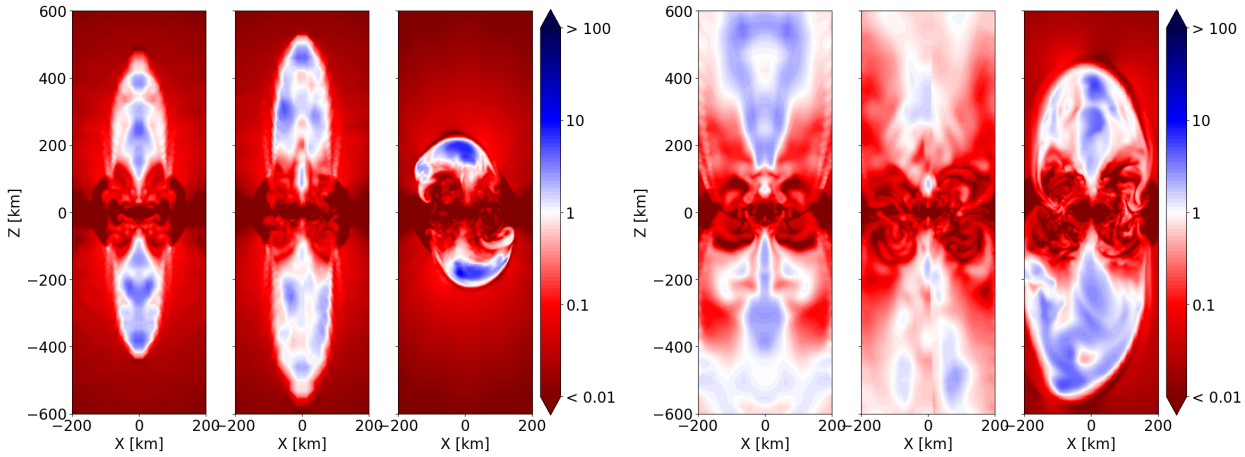

Fig. 2. Left: 2D map of the inverse plasma beta at $t = 50$ ms p.b. for a 2D and 3D model produced with `AENUS-ALCAR` (left and mid panel) and the 3D model by `FLASH-M1` (right). **Right:** Same as the adjacent panel, but at $t = 100$ ms p.b.

2.1 Results

2.2 Explosion dynamics and proto-neutron star formation

As shown in Fig. 1, all simulations lead to prompt magneto-rotational explosions (regardless of the code employed or their dimensionality) having, however, different degrees of efficiency. `AENUS-ALCAR` produces produces the fastest shock expansion (left panel) and the most energetic ejecta (right panel), while the 3D model obtained with `3DnSNe-IDSA` shows a slower onset of the explosion. For these two codes there is also a different trend with the problem's dimensions: 3D explosions are more powerful that the axisymmetric counterpart for `AENUS-ALCAR`, whereas the opposite is true for `3DnSNe-IDSA`. The ejecta energy increases at a similar rate for all models, with a time offset due to the specific time of the onset of the explosion.

The mass of the forming proto-neutron star (PNS) is consistently reproduced over time by all codes, as it is the toroidal magnetic energy up to $t \sim 150$ ms p.b. The total rotational energy of the PNS tends to be higher in the `CoCoNuT-FMT` and `3DnSNe-IDSA` models (up to $\sim 30\%$), which my be connected to the approximated treatment of the PNS inner part (assumed to be spherically symmetric). Overall, the radial profiles of density, entropy, and the magnetic field components are consistently reproduced by all codes.

2.3 The kink instability

Besides the different explosion energies, the outflows produced by our 3D simulations display also different degrees of collimation and morphology. Fig. 2 shows how the `AENUS-ALCAR` 3D model has a rather axisymmetric structure, while the explosion produced with `FLASH-M1` has clear non-axisymmetric features and north-south asymmetries. Interestingly, the latter model has also a higher ratio of magnetic to thermal pressure, although it leads to a weaker explosion than the `AENUS-ALCAR`'s one.

To characterize the development of the kink instability, we track the evolution of the outflows barycenter at different altitudes $z = \pm\{50, 100, 500\}$ km. We consider the horizontal planes passing through each value of z and define the barycenter's Cartesian coordinates as (Mösta et al. 2014)

$$x_c^i = \frac{\int_{s<z} x^i P_{\rm mag}\, \mathrm{d}s}{\int_{s<z} P_{\rm mag}\, \mathrm{d}s}, \tag{2.3}$$

where $x^i = \{x, y\}$ are the Cartesian coordinates of each point in the plane, $P_{\rm mag} = B^2/8\pi$ is the local magnetic pressure and the averages extend to a distance from the rotational axis z.

In Fig. 3 we report the jet barycenter displacement for the `AENUS-ALCAR` and `FLASH-M1` models (with and without initial perturbations) at a distance of 100 km from the center of the PNS. For both codes there is an exponential growth of the displacement, which however saturates within $\sim$25 ms to roughly 10% of its vertical altitude. This shows that there is no ultimate disruption of the outflow due to the kink instability within the duration of our simulations, but rather a quantitative decrease in its collimation.

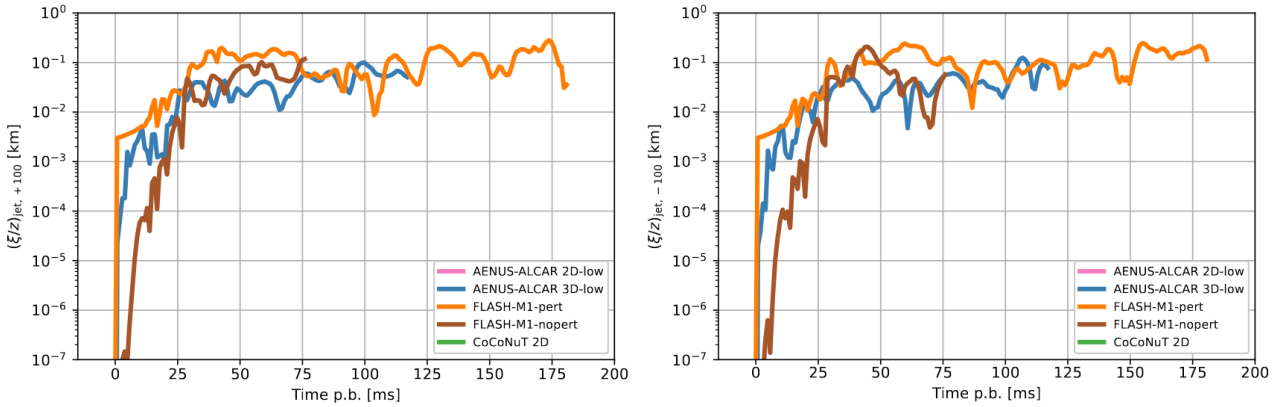

Fig. 3. Left: Northern jet's barycenter displacement in units of the vertical distance from the center (100 km) as a function of time **Right:** Same as the adjacent panel, but for the southern jet.

3 Conclusions

We presented results from a comparison study of 2D and 3D numerical models of magneto-rotational core-collapse supernovae performed with four different state-of-the-art codes. Our results show that, starting from the same stellar progenitor and initial conditions, different codes can lead to qualitatively similar explosions within the first $\sim$ 100 ms after shock formation. However, we also measured quantitative deviations in the explosion efficiency and shock radius expansion, whose source needs to more thoroughly be investigated. The PNS mass is consistently reproduced by all models, but there are differences in its rotation rates and total angular momentum which are likely tied to the differences in explosion efficiencies. We found no ultimate disruption of the outflow by the kink instability, but different models can exhibit distinctive variations in the azimuthal structure of the outflow.

References

Aloy, M. Á. & Obergaulinger, M. 2021, Monthly Notices of the Royal Astronomical Society, 500, 4365
Bugli, M., Guilet, J., Foglizzo, T., & Obergaulinger, M. 2023, MNRAS, 520, 5622
Bugli, M., Guilet, J., & Obergaulinger, M. 2021, MNRAS, 507, 443, aDS Bibcode: 2021MNRAS.507..443B
Bugli, M., Guilet, J., Obergaulinger, M., Cerdá-Durán, P., & Aloy, M. A. 2020, MNRAS, 492, 58
Just, O., Obergaulinger, M., & Janka, H.-T. 2015, MNRAS, 453, 3386
Kuroda, T., Arcones, A., Takiwaki, T., & Kotake, K. 2020, arXiv:2003.02004 [astro-ph], arXiv: 2003.02004
Kuroda, T. & Umeda, H. 2010, The Astrophysical Journal Supplement Series, 191, 439
Marek, A., Dimmelmeier, H., Janka, H.-T., Müller, E., & Buras, R. 2006, Astronomy & Astrophysics, 445, 273
Müller, B., Dimmelmeier, H., & Müller, E. 2008, Astronomy & Astrophysics, 489, 301
Müller, B. & Janka, H.-T. 2015, Monthly Notices of the Royal Astronomical Society, 448, 2141
Mösta, P., Richers, S., Ott, C. D., et al. 2014, The Astrophysical Journal, 785, L29, citation Key Alias: mosta2014a
Obergaulinger, M. & á. Aloy, M. 2017, Monthly Notices of the Royal Astronomical Society: Letters, 469, L43
O'Connor, E. P. & Couch, S. M. 2018, The Astrophysical Journal, 854, 63
Powell, J., Müller, B., Aguilera-Dena, D. R., & Langer, N. 2023, MNRAS, 522, 6070
Reichert, M., Bugli, M., Guilet, J., et al. 2024, Monthly Notices of the Royal Astronomical Society
Reichert, M., Obergaulinger, M., Aloy, M. Á., et al. 2022, MNRAS, 518, 1557
Shibagaki, S., Kuroda, T., Kotake, K., Takiwaki, T., & Fischer, T. 2024, MNRAS, 531, 3732
Takiwaki, T., Kotake, K., & Sato, K. 2009, The Astrophysical Journal, 691, 1360
Takiwaki, T., Kotake, K., & Suwa, Y. 2016, MNRASL, 461, L112
Woosley, S. & Heger, A. 2007, Physics Reports, 442, 269
Zha, S., Müller, B., & Powell, J. 2024, arXiv:2403.02072